Appl. Math. Mech. -Engl. Ed., **35**(2), 155–166 (2014)
DOI 10.1007/s10483-014-1780-8

Applied Mathematics and Mechanics (English Edition)

Mixed convection stagnation-point flow on vertical stretching sheet with external magnetic field*

F. M. ALI[1], R. NAZAR[2], N. M. ARIFIN[1], I. POP[3]

(1. Department of Mathematics & Institute for Mathematical Research, Universiti Putra Malaysia, UPM Serdang 43400, Selangor, Malaysia;
2. School of Mathematical Sciences, Faculty of Science & Technology, Universiti Kebangsaan Malaysia, UKM Bangi 43600, Selangor, Malaysia;
3. Department of Mathematics, Babeş-Bolyai University, Cluj-Napoca R-400084, Romania)

Abstract The problem of steady laminar magnetohydrodynamic (MHD) mixed convection stagnation-point flow of an incompressible viscous fluid over a vertical stretching sheet is studied. The effect of an externally magnetic field is taken into account. The transformed boundary layer equations are solved numerically by using an implicit finite-difference scheme. Numerical results are obtained for various values of the mixed convection parameter, Hartmann number, and Prandtl number. The effects of an externally magnetic field on the skin friction coefficient, local Nusselt number, velocity, and temperature profiles for both $A > 1$ and $A < 1$, where A is the velocity ratio parameter, are presented graphically and discussed in detail. Both assisting and opposing flows are considered, and it is found that dual solutions exist for the opposing flow.

Key words boundary layer, mixed convection, magnetohydrodynamic (MHD), numerical result, stagnation-point, stretching sheet

Chinese Library Classification O345
2010 Mathematics Subject Classification 76D10, 76W05

1 Introduction

Study of boundary layer flow and heat transfer over stretching sheet has attracted many researchers. Ahmad et al.[1] investigated the heat transfer problem with variable thermal conductivity in the case of prescribed surface temperature and prescribed heat flux. Further, Kumari and Nath[2] considered the unsteady magnetohydrodynamic (MHD) mixed convection flow over an impulsively stretched permeable vertical surface in the presence of a transverse uniform magnetic field. Prasad et al.[3] studied the mixed convection boundary layer flow over a vertical heated sheet with variable fluid properties, while Ali et al.[4] investigated the MHD boundary layer flow over a stretching sheet with the effect of induced magnetic field.

* Received Nov. 7, 2012 / Revised Aug. 23, 2013
Project supported by the Fundamental Research Grant Scheme (FRGS) from the Ministry of Higher Education in Malaysia (No. 5524295), and the Research University Grant from the Universiti Kebangsaan Malaysia (No. GUP-2013-040)
Corresponding author F. M. ALI, Ph. D., E-mail: fadzilahma@upm.edu.my

On the other hand, the fluid flow near a stagnation-point has many practical applications in engineering such as the cooling of nuclear reactors and hydrodynamic processes. It is worth mentioning that Hiemenz[5] obtained an exact similarity solution of the Navier-Stokes equations for two-dimensional stagnation-point flow. Later, Eckert[6] extended this idea by considering the energy equation in his study. Further, Mahapatra and Gupta[7] investigated the heat transfer in the stagnation-point flow towards a stretching sheet without consideration of MHD and found that the boundary layer structure depends on the ratio of the velocity of the stretching surface to that of the frictionless potential flow near the stagnation-point. In non-Newtonian fluids, Andersson[8] obtained an exact solution for MHD flow past a stretching sheet in the presence of a transverse magnetic field in a viscoelastic fluid. Ishak et al.[9] considered the MHD flow of a micropolar fluid towards a stagnation point on a vertical surface, while Mahapatra et al.[10] studied the MHD stagnation-point flow of a power-law fluid towards a stretching sheet. The MHD boundary layer flow and heat transfer over a stretching sheet with Hall effects has also been investigated by Gupta et al.[11] and Ali et al.[12], while Ishak et al.[13] considered the hydromagnetic flow and heat transfer adjacent to a vertical stretching sheet. On the other hand, papers by Pop et al.[14] and Pal[15] included the thermal radiation effects, while paper by Hayat et al.[16] considered the case of micropolar fluid for a nonlinear stretching surface. No dual solutions have been reported in all the papers[7–16].

The flow and heat transfer characteristics in the boundary layer induced by a continuous surface moving with a uniform or non-uniform velocity in a quiescent fluid are important in several manufacturing processes in industry such as the extrusion of a plastic sheet, the cooling of a metallic plate in a cooling bath, wire drawing, and hot rolling. Glass blowing, fibre production, crystal growing, and paper production also involve the flow due to a stretching surface. This problem differs from the classical boundary layer flow over a stationary surface due to the entrainment of the fluid[2]. A moving surface delays or prevents the separation of boundary layer from the wall by importing momentum into the boundary layer[17]. The buoyancy force, suction or injection, and the magnetic field significantly influence the skin friction and heat transfer. In recent years, MHD problems have become important industrially. Many metallurgical processes, such as drawing, annealing, and tinning of copper wires involve the cooling of continuous strip or filaments by drawing them through a quiescent fluid. By drawing such strips in an electrically conducting fluid subjected to a magnetic field, the rate of cooling can be controlled and a final product of desired quality can be obtained. Another important application of hydromagnetics to metallurgy is the purification of molten metals from non-metallic inclusions by the application of a magnetic field. Therefore, the MHD mixed convection flow over a vertical stretched surface in the presence of a magnetic field is an important problem[2].

Convective heat transfer in an electrically conducting fluid at a stretching surface with uniform free stream has been considered by Vajravelu and Hadijinicolaou[18], while the explicit analytic solution for the problem has been considered by Xu[19]. On the other hand, Ishak et al.[20] considered the steady MHD stagnation-point flow towards a stretching sheet with variable surface temperature, and Bachok et al.[21] studied the anisotropy effect in a porous medium. The present paper aims to study the problem of MHD mixed convection stagnation-point flow and heat transfer towards a stretching vertical sheet with externally magnetic field. The transformed equations are solved numerically by using an efficient implicit finite-difference method. To the best of our knowledge, this specific problem has not been considered before. Therefore, the reported results are original and new.

2 Basic equations

Consider the steady two-dimensional flow of a viscous fluid near the stagnation-point on a vertical stretching flat plate coinciding with the plane $y = 0$, as shown in Fig. 1. Cartesian coordinates (x, y) are taken such that the x-axis is measured along the sheet oriented in the

upward direction, and the y-axis is normal to it. It is assumed that the velocity of the far-flow (inviscid flow) impinges on the stretching surface with the velocity $u_{\rm e}(x) = ax$ and that the flat surface is stretched with the velocity $u_{\rm w}(x) = cx$, where a and c are positive constants. It is also assumed that the temperature of the plate is $T_{\rm w}(x) = T_\infty + bx$, where T_∞ is the temperature of the ambient fluid, while b is a constant with $b > 0$ for a heated surface $T_{\rm w}(x) > T_\infty$ (assisting flow) and $b < 0$ for a cooled surface $T_{\rm w}(x) < T_\infty$ (opposing flow). The assisting flow occurs if the upper half of the sheet is heated while the lower half of the sheet is cooled. In this case, the flow near the heated sheet tends to move upward and the flow near the cooled sheet tends to move downward. Therefore, this behavior acts to assist the flow field. The opposing flow occurs if the upper part of the sheet is cooled while the lower part of the sheet is heated. These flows are illustrated in Fig. 1(a) for the assisting flow and in Fig. 1(b) for the opposing flow.

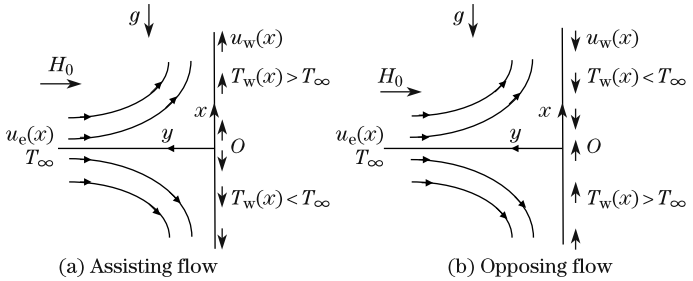

Fig. 1 Physical model and coordinate system

The effect of an external magnetic field of constant strength H_0, which is applied normal to the stretching surface, is also taken into account. Under these assumptions, together with the Boussinesq approximations and neglecting the viscous dissipation effect, the steady two-dimensional flow of a viscous and electrically conducting fluid is described by the following equations:

$$\frac{\partial u}{\partial x} + \frac{\partial v}{\partial y} = 0, \tag{1}$$

$$u\frac{\partial u}{\partial x} + v\frac{\partial u}{\partial y} = -\frac{1}{\rho}\frac{{\rm d}p}{{\rm d}x} + \nu\frac{\partial^2 u}{\partial y^2} - \frac{\sigma_{\rm e}\mu_{\rm e}^2 H_0^2}{\rho}u + g\beta(T - T_\infty), \tag{2}$$

$$u\frac{\partial T}{\partial x} + v\frac{\partial T}{\partial y} = \alpha\frac{\partial^2 T}{\partial y^2}, \tag{3}$$

where u and v are the velocity components along the x- and y-axes, respectively, p is the pressure, T is the fluid temperature, g is the acceleration due to gravity, and α, ν, ρ, β, $\sigma_{\rm e}$, and $\mu_{\rm e}$ are the thermal diffusivity, kinematic viscosity, fluid density, thermal expansion coefficient, electrical conductivity, and magnetic permeability, respectively. The boundary conditions of Eqs. (1)–(3) are

$$\begin{cases} v = 0, \quad u = u_{\rm w}(x) = cx, \quad T = T_{\rm w}(x) = T_\infty + bx \quad \text{at} \quad y = 0, \\ u = u_{\rm e}(x) = ax, \quad T = T_\infty \quad \text{as} \quad y \to \infty. \end{cases} \tag{4}$$

In this study, the induced magnetic field has been ignored. For the most general model of practical importance, the forces due to the hydrostatic and magnetic pressure gradient would be in equilibrium (see Sutton and Sherman[22]), namely,

$$-\frac{1}{\rho}\frac{{\rm d}p}{{\rm d}x} = u_{\rm e}\frac{{\rm d}u_{\rm e}}{{\rm d}x} + \frac{\sigma\mu_{\rm e}^2 H_0^2}{\rho}u_{\rm e}, \tag{5}$$

because $T = T_\infty$ in the inviscid (outer boundary layer) flow. By substituting Eq. (5) into Eq. (2), we obtain the following boundary layer equation:

$$u\frac{\partial u}{\partial x} + v\frac{\partial u}{\partial y} = u_\mathrm{e}\frac{\mathrm{d}u_\mathrm{e}}{\mathrm{d}x} + \nu\frac{\partial^2 u}{\partial y^2} - \frac{\sigma_\mathrm{e}\mu_\mathrm{e}^2 H_0^2}{\rho}(u - u_\mathrm{e}) + g\beta(T - T_\infty). \tag{6}$$

We apply the following transformation:

$$\psi = x\sqrt{a\nu}f(\eta), \quad \theta(\eta) = (T - T_\infty)/(T_\mathrm{w} - T_\infty), \quad \eta = \sqrt{a/\nu}\, y \tag{7}$$

to Eqs. (1), (3), and (6), where ψ is the stream function, which is defined in the usual way as $u = \frac{\partial \psi}{\partial y}$ and $v = -\frac{\partial \psi}{\partial x}$. Therefore, the continuity equation (1) is satisfied, and Eqs. (6) and (3) are reduced to the following nonlinear ordinary differential equations:

$$f''' + ff'' - (f')^2 + 1 + Ha^2(1 - f') + \lambda\theta = 0, \tag{8}$$

$$\frac{1}{Pr}\theta'' + f\theta' - f'\theta = 0, \tag{9}$$

and the boundary conditions (4) become

$$f(0) = 0, \quad f'(0) = A, \quad \theta(0) = 1, \quad f'(\infty) = 1, \quad \theta(\infty) = 0. \tag{10}$$

Here, primes denote differentiation with respect to η, $A = c/a$ is the velocity ratio parameter, $Ha = \mu_\mathrm{e}H_0\sqrt{\sigma_\mathrm{e}/\rho a}$ is the Hartmann number, $Pr = \nu/\alpha$ is the Prandtl number, and λ is the constant mixed convection or buoyancy parameter, which is defined as

$$\lambda = \frac{Gr_x}{Re_x^2}, \tag{11}$$

where $Gr_x = g\beta(T_\mathrm{w} - T_\infty)x^3/\nu^2$ is the local Grashof number, and $Re_x = u_\mathrm{e}(x)x/\nu$ is the local Reynolds number. It would be mentioned that $\lambda > 0$ corresponds to the assisting flow, $\lambda < 0$ corresponds to the opposing flow, and $\lambda = 0$ corresponds to the forced convection flow. Further, it would be noticed that for a static surface ($A = 0$) and without a magnetic field ($Ha = 0$), the present problem reduces to that first studied by Ramachandran et al.[23]. Thus, we can also compare our results with those reported by Ramachandran et al.[23].

The physical quantities of interest are the skin friction coefficient C_f and the local Nusselt number Nu_x, which are defined as

$$C_\mathrm{f} = \frac{\tau_\mathrm{w}}{\frac{1}{2}\rho u_\mathrm{e}^2}, \quad Nu_x = \frac{xq_\mathrm{w}}{k(T_\mathrm{w} - T_\infty)}, \tag{12}$$

where the surface shear stress τ_w and the surface heat flux q_w are given by

$$\tau_\mathrm{w} = \mu\Big(\frac{\partial u}{\partial y}\Big)_{y=0}, \quad q_\mathrm{w} = -k\Big(\frac{\partial T}{\partial y}\Big)_{y=0}, \tag{13}$$

where k is the thermal conductivity, and μ is the dynamic viscosity. Using variables in (12), we obtain

$$Re_x^{1/2}C_\mathrm{f} = f''(0), \quad Re_x^{-1/2}Nu_x = -\theta'(0). \tag{14}$$

3 Results and discussion

Equations (8) and (9) subjected to the boundary conditions (10) have been solved numerically by an implicit finite-difference scheme known as the Keller-box method as described by Cebeci and Bradshaw[24] and Cebeci and Cousteix[25]. In order to check the validity of the obtained numerical results, the values of the skin friction coefficient $f''(0)$ and the local Nusselt number $-\theta'(0)$ for the static case ($A = 0$) when the Hartmann number is absent ($Ha = 0$) and the mixed convection parameter $\lambda = 1$, are compared with the previously published results[23,26–28] as shown in Tables 1 and 2. The agreement is found to be very good. Further, Tables 3 and 4 show the comparison values of the skin friction coefficient $f''(0)$ and the local Nusselt number $-\theta'(0)$ for various Prandtl number Pr and both assisting and opposing flows are considered. The agreement with previously published results[29] is also found to be excellent. The effects of Ha on the skin friction coefficient $f''(0)$ for the assisting and opposing flows when $A = 2$ and $Pr = 0.7$ are shown in Table 5. It is observed that all values of $f''(0)$ and $-\theta'(0)$ decrease when Ha increases for both assisting ($\lambda = 2$) and opposing ($\lambda = -2$) flows. The case of $A < 1$ ($A = 0.5$) is displayed in Table 6, where the opposite phenomenon can be observed. From both tables, it can be seen that all values for the assisting flow are always larger than those for the opposing flow case. This occurs due to the buoyancy parameter that assists the flow.

Table 1 Skin friction coefficient $f''(0)$ for different values of Pr when $\lambda = 1$, $A = 0$, and $Ha = 0$ (values in ( ) are second solutions)

Pr	Ramachandran et al.[23]	Hassanien and Gorla[26]	Lok et al.[27]	Ishak et al.[28]	Present
0.7	1.706 3	1.706 3	1.706 4	1.706 3 (1.238 7)	1.706 3 (1.238 8)
1	—	—	—	1.675 4 (1.133 2)	1.675 4 (1.133 2)
7	1.517 9	—	1.518 0	1.517 9 (0.582 4)	1.517 9 (0.582 4)
10	—	1.492 8	—	1.492 8 (0.495 8)	1.492 9 (0.495 8)
20	1.448 5	—	1.448 6	1.445 0 (0.343 6)	1.448 5 (0.343 6)
40	1.410 1	—	1.410 2	1.410 1 (0.211 1)	1.410 1 (0.211 1)
50	—	1.406 9	—	1.398 9 (0.172 0)	1.398 9 (0.172 1)
60	1.390 3	—	1.390 3	1.390 3 (0.141 3)	1.390 3 (0.141 3)
80	1.377 4	—	1.377 3	1.377 4 (0.094 7)	1.377 4 (0.094 7)
100	1.368 0	1.384 7	1.367 7	1.368 0 (0.060 1)	1.368 0 (0.060 1)

Table 2 Local Nusselt number $-\theta'(0)$ for different values of Pr when $\lambda = 1$, $A = 0$, and $Ha = 0$ (values in ( ) are second solutions)

Pr	Ramachandran et al.[23]	Hassanien and Gorla[26]	Lok et al.[27]	Ishak et al.[28]	Present
0.7	0.764 1	1.764 1	0.764 1	0.764 1 (1.022 6)	0.764 1 (1.022 6)
1	—	—	—	0.870 8 (1.169 1)	0.870 8 (1.169 1)
7	1.722 4	—	1.722 6	1.722 4 (2.219 2)	1.722 5 (2.219 1)
10	—	1.944 6	—	1.944 6 (2.494 0)	1.944 8 (2.494 0)
20	2.457 6	—	2.457 7	2.457 6 (3.164 6)	2.457 9 (3.164 4)
40	3.101 1	—	3.102 3	3.101 1 (4.108 0)	3.101 7 (4.107 6)
50	—	3.348 8	—	3.341 5 (4.497 6)	3.342 3 (4.497 0)
60	3.551 4	—	3.556 0	3.551 4 (4.857 2)	3.552 4 (4.856 4)
80	3.909 5	—	3.919 5	3.909 5 (5.516 6)	3.910 8 (5.515 5)
100	4.211 6	4.233 7	4.228 9	4.211 6 (6.123 0)	4.213 3 (6.121 5)

Table 3 Skin friction coefficient $f''(0)$ and local Nusselt number $-\theta'(0)$ for different values of Pr when $A = 1$, $Ha = 0$, and $\lambda = 1$ (assisting flow)

Pr	Ishak et al.[29]		Present	
	$f''(0)$	$-\theta'(0)$	$f''(0)$	$-\theta'(0)$
0.72	0.364 5	1.093 1	0.364 5	1.093 1
6.8	0.180 4	3.290 2	0.180 4	3.289 7
20	0.117 5	5.623 0	0.117 5	5.620 8
40	0.087 3	7.946 3	0.087 3	7.940 3
60	0.072 9	9.732 7	0.072 9	9.721 7
80	0.064 0	11.241 3	0.064 0	11.224 4
100	0.057 8	12.572 6	0.057 8	12.549 0

Table 4 Skin friction coefficient $f''(0)$ and local Nusselt number $-\theta'(0)$ for different values of Pr when $A = 1$, $Ha = 0$, and $\lambda = -1$ (opposing flow)

Pr	Ishak et al.[29]		Present	
	$f''(0)$	$-\theta'(0)$	$f''(0)$	$-\theta'(0)$
0.72	−0.385 2	1.029 3	−0.385 2	1.029 3
6.8	−0.183 2	3.246 6	−0.183 2	3.246 2
20	−0.118 3	5.592 3	−0.118 3	5.590 3
40	−0.087 6	7.922 7	−0.087 6	7.916 9
60	−0.073 1	9.712 6	−0.073 1	9.701 8
80	−0.064 2	11.223 5	−0.064 1	11.206 8
100	−0.057 9	12.556 4	−0.057 9	12.532 9

Table 5 Skin friction coefficient $f''(0)$ and local Nusselt number $-\theta'(0)$ for different values of Ha when $A = 2$ and $Pr = 0.7$ for assisting ($\lambda = 2$) and opposing ($\lambda = -2$) flows

Ha	Assisting flow		Opposing flow	
	$f''(0)$	$-\theta'(0)$	$f''(0)$	$-\theta'(0)$
0	−1.274 6	1.346 6	−2.541 7	1.264 2
1	−1.555 1	1.330 9	−2.740 7	1.256 0
2	−2.243 5	1.296 8	−3.259 3	1.237 5
5	−5.030 6	1.208 5	−5.649 7	1.182 4
10	−9.996 1	1.143 2	−10.351 4	1.133 2

Table 6 Skin friction coefficient $f''(0)$ and local Nusselt number $-\theta'(0)$ for different values of Ha when $A = 0.5$ and $Pr = 0.7$ for assisting ($\lambda = 2$) and opposing ($\lambda = -2$) flows

Ha	Assisting flow		Opposing flow	
	$f''(0)$	$-\theta'(0)$	$f''(0)$	$-\theta'(0)$
0	1.509 6	0.965 3	−0.234 0	0.781 2
1	1.584 2	0.965 8	0.075 2	0.824 6
2	1.800 5	0.969 4	0.624 9	0.879 2
5	2.920 2	0.987 8	2.274 1	0.957 6
10	5.229 6	1.008 1	4.869 8	0.998 3

In this study, dual solutions are obtained for the opposing flow regime, while a unique solution is obtained for the assisting flow regime. This can be seen clearly from Figs. 2 and 3 for different values of Hartmann number when $Pr = 0.7$ and $A = 2$. It is observed that $f''(0)$ and $-\theta'(0)$ have no solution when $\lambda < |\lambda_c|$ (critical value). Therefore, the boundary layer

starts to separate from the surface at $\lambda = \lambda_c$. Beyond this critical point, boundary layer approximations are no longer valid and full Navier-Stokes equations have to be considered. Both figures show that the critical value λ_c increases as the parameter Ha increases. Thus, larger values of Hartmann number delay the boundary layer separation. The coordinates of the critical (turning) points are shown in Table 7.

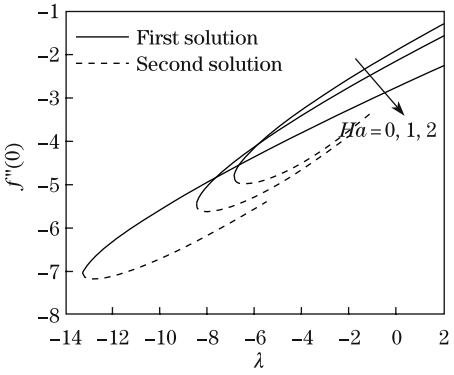

Fig. 2 Skin friction coefficient $f''(0)$ as function of λ for different values of Ha when $Pr = 0.7$ and $A = 2$

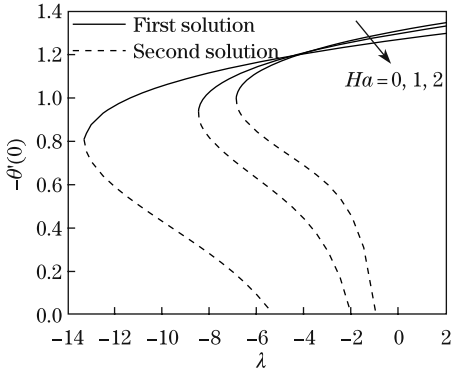

Fig. 3 Local Nusselt number $-\theta'(0)$ as function of λ for different values of Ha when $Pr = 0.7$ and $A = 2$

Table 7 Coordinates of critical (turning) points in Fig. 2 for $Ha = 0$, 1, and 2

Ha	0	1	2
$(\lambda, f''(0))$	$(-6.885, -4.792\,8)$	$(-8.475, -5.495\,3)$	$(-13.295, -7.023\,9)$
$(\lambda, -\theta'(0))$	$(-6.885, 0.997\,6)$	$(-8.475, 0.924\,1)$	$(-13.295, 0.815\,1)$

Figures 4 and 5 show the dual velocity and temperature profiles (first and second branch solutions), respectively, for a fixed Hartmann number, namely, $Ha = 2$, $Pr = 0.7$, and $A = 2$ for different values of λ. These first and second branch profiles prove the existence of the dual nature of solutions as they satisfy the boundary conditions (10). Between the two solutions, which solution is physically relevant depends essentially on the stability of the solutions. As in similar physical situations, we expect that one solution is physically stable, while the other is not. However, the problem of determining the physically realizable solution of the multiple (dual) solutions implies a separate study by considering the unsteady form of Eqs. (1) to (3). Such stability analysis can also be found in a very recently published paper by Rosca and Pop[30]. Therefore, it can be easily concluded from this paper that the lower branch solutions are unstable (not realizable physically), while the upper branch solutions are stable (physically realizable). It seems that the existence of dual solutions in the mixed convection boundary layer flow was first pointed out by Merkin[31–32] for the steady mixed convection boundary layer flow over a vertical flat plate embedded in a porous medium. Dual solutions in the mixed convection boundary layer flow were further studied by Hoog et al.[33], Afzal and Hussain[34], and Harris et al.[35]. As discussed by Afzal and Hussain[34], it seems plausible that depending on the manner in which the temperature field is imposed, one or the other dual solutions could be approached after different adjustment phases, causing the solution in the neighborhood of the separation region to be dual. Such dual solutions for MHD two-dimensional stagnation-point flow past a vertical stretching surface have not been reported in the literature.

Figure 6 shows the velocity profiles for different values of A for fixed $\lambda = 1$, $Ha = 1$, and $Pr = 0.7$. In the case of $A < 1$, the flow shows a boundary layer structure, while when $A > 1$, the flow displays an inverted boundary layer structure as a result of the stretching velocity

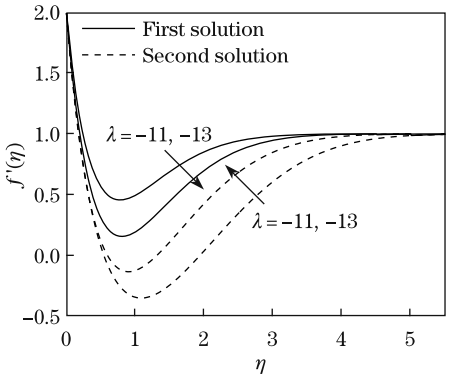

Fig. 4 Velocity profiles for different values of λ when $Ha = 2$, Pr=0.7, and A=2

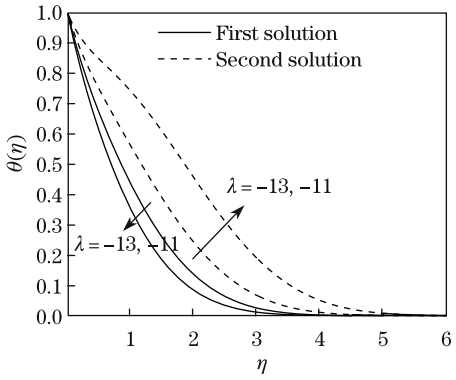

Fig. 5 Temperature profiles for different values of λ when $Ha = 2$, Pr=0.7, and A=2

of the surface exceeds the velocity of the free stream. It is also seen that as A increases, the boundary layer thickness decreases as illustrated in Fig. 6. The effects of Ha on the velocity profiles are displayed in Fig. 7. Larger values of Ha are found to decrease the velocity profiles when $A > 1$, hence thinning the boundary layer thickness for both assisting and opposing flows. The velocity gradient becomes smaller, which decreases the skin friction coefficient, as shown in Table 5. When $A < 1$, the velocity profiles increase with Ha for the assisting and opposing flows, and the velocity gradient becomes larger. The effects of Pr and λ on the velocity profiles are shown in Figs. 8 and 9, respectively. The effects are more pronounced for lower Pr and larger λ. Larger values of λ will produce larger buoyancy force, which produce larger kinetic energy, which helps to reduce resistant of the fluid flow. Both figures show that the profiles are prominent when $A < 1$ is considered. Figure 8 shows that as Pr increases, the velocity profiles decrease when both $A > 1$ and $A < 1$ are considered for the assisting flow. On the other hand, opposite trend is found in the opposing flow. Reversed phenomenon occurs for the buoyancy parameter, as shown in Fig. 9. Boundary layer structure and inverted boundary layer structure can be seen in Figs. 6–9, where the boundary layer thickness when $A < 1$ is always larger than the thickness when $A > 1$, and also larger for the opposing flow.

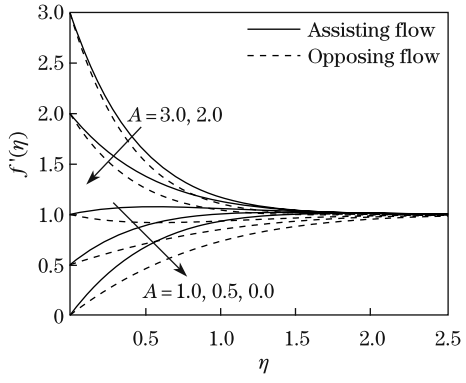

Fig. 6 Velocity profiles for different values of A when Pr=0.7 and $Ha = 1$ for $\lambda = 1$ (assisting flow) and $\lambda = -1$ (opposing flow)

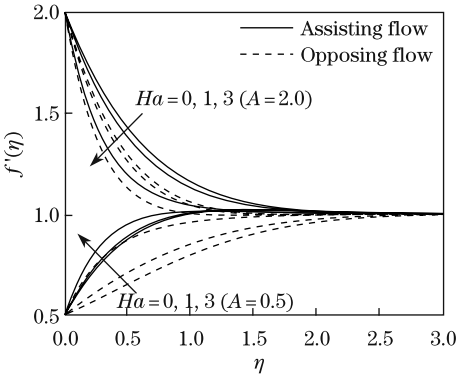

Fig. 7 Velocity profiles for different values of Ha when Pr=0.7, $A = 0.5$, and $A = 2$ for $\lambda = 1$ (assisting flow) and $\lambda = -1$ (opposing flow)

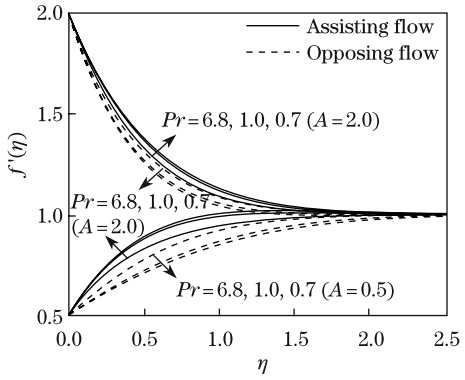

Fig. 8 Velocity profiles for different values of Pr when $Ha = 1$, $A = 0.5$, and $A = 2$ for $\lambda = 1$ (assisting flow) and $\lambda = -1$ (opposing flow)

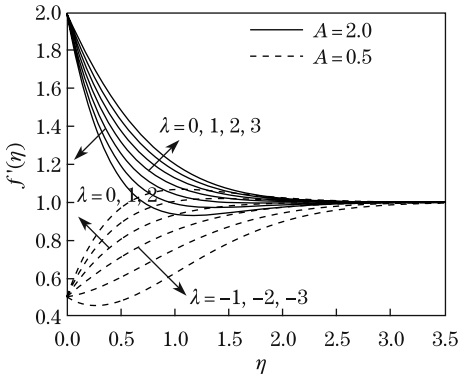

Fig. 9 Velocity profiles for different values of λ when Pr=0.7, $Ha = 1$, $A = 0.5$, and $A = 2$

Figure 10 shows the influence of A on the temperature profiles. The temperature profiles are observed to reduce as A increases, as well as the thermal boundary layer thickness for both assisting and opposing flows. Figures 11 and 12 show the effects of Ha on the temperature profiles. The effects of Ha on the temperature profiles are not prominent for both $A < 1$ and $A > 1$. The temperature profiles increase with Ha when $A > 1$ and $A < 1$, for both assisting and opposing flows.

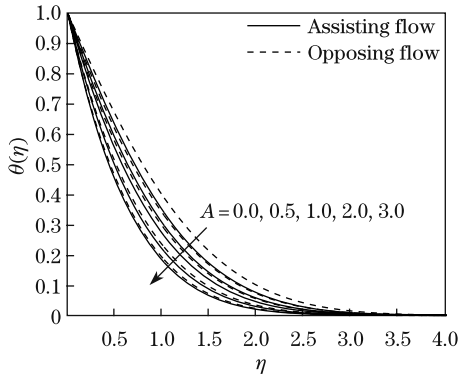

Fig. 10 Temperature profiles for different values of A when $Ha = 1$ and $Pr = 0.7$ for $\lambda = 1$ (assisting flow) and $\lambda = -1$ (opposing flow)

The temperature profiles are found to decrease with Pr for both $A < 1$ and $A > 1$, as shown in Figs. 13 and 14, respectively. This illustrates that for larger Pr, it leads to the decrease of the temperature profiles and the thermal boundary layer thickness becomes smaller. This phenomenon occurs because when Pr increases and the thermal diffusivity decreases, thus it leads to the decrease of energy transfer ability that decreases the thermal boundary layer. The effects of the buoyancy parameter on the temperature profiles can be seen from Figs. 15–16. In the assisting flow, larger values of λ reduce the profiles for both $A > 1$ and $A < 1$. An opposite phenomenon occurs in the opposing flow. The effect of λ is not pronounced when $A > 1$ is considered. The thermal boundary layer thickness for the opposing flow is always greater as compared with the assisting flow for both $A > 1$ and $A < 1$. This can be observed from Figs. 10–16.

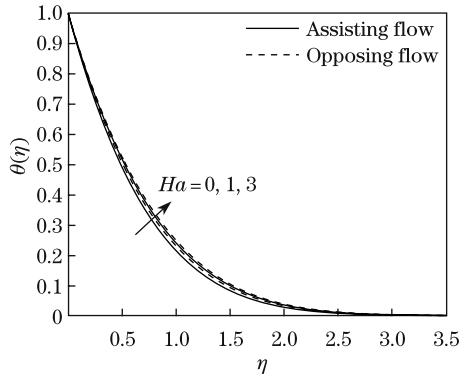

Fig. 11 Temperature profiles for different values of Ha when $Pr = 0.7$ and $A = 0.5$ for $\lambda = 1$ (assisting flow) and $\lambda = -1$ (opposing flow)

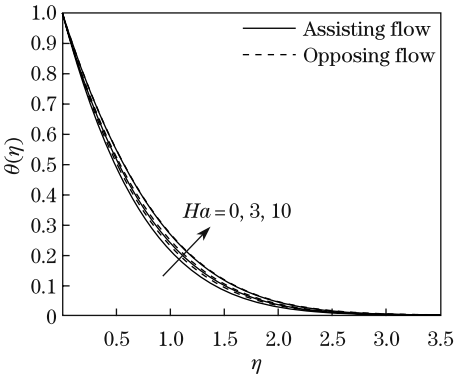

Fig. 12 Temperature profiles for different values of Ha when Pr=0.7 and $A = 2.0$ for $\lambda = 1$ (assisting flow) and $\lambda = -1$ (opposing flow)

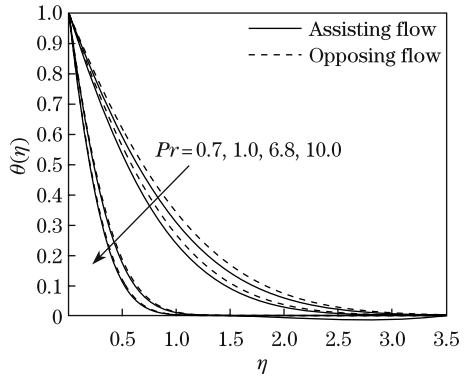

Fig. 13 Temperature profiles for different values of Pr when Ha=1 and $A = 0.5$ for $\lambda = 1$ (assisting flow) and $\lambda = -1$ (opposing flow)

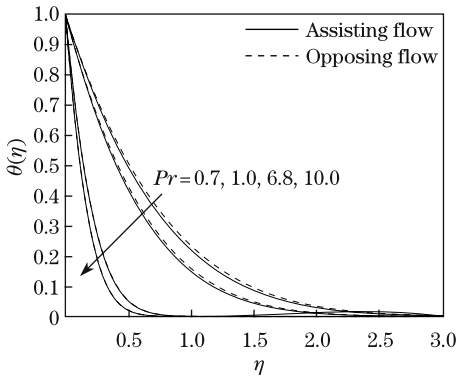

Fig. 14 Temperature profiles for different values of Pr when $Ha = 1$ and $A = 2$ for $\lambda = 1$ (assisting flow) and $\lambda = -1$ (opposing flow)

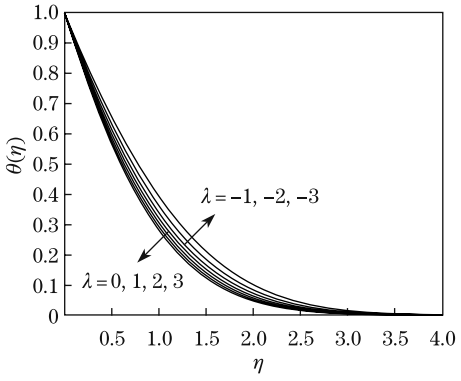

Fig. 15 Temperature profiles for different values of λ when $Pr = 0.7$, $Ha = 1$, and $A = 0.5$

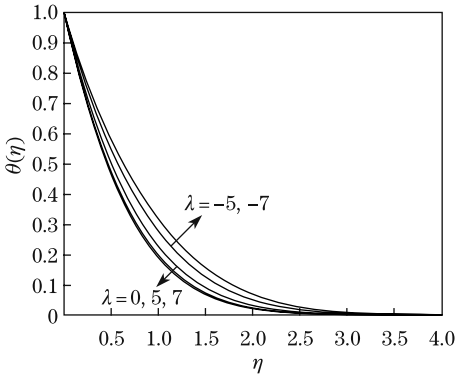

Fig. 16 Temperature profiles for different values of λ when $Pr = 0.7$, $Ha = 1$, and $A = 2$

4 Conclusions

A numerical study is performed for the problem of MHD mixed convection stagnation-point flow of an incompressible viscous fluid over a vertical stretching sheet in the presence of an externally magnetic field. The results obtained are compared with previous well-known results for special cases, and the agreement is excellent. It is observed that when $A > 1$, all the skin friction coefficient and the local Nusselt number decrease as Ha increases for both assisting and opposing flows, while opposite trend can be observed for $A < 1$. For the assisting flow, it is observed that when $A < 1$, the flow has a boundary layer structure and when $A > 1$, an inverted boundary layer structure is observed. The boundary layer thickness when $A < 1$ is always larger than that when $A > 1$. This is also applied to a larger values of the opposing flow. The thermal boundary layer thickness for the opposing flow is always greater compared with the assisting flow for both $A > 1$ and $A < 1$. The effects are more pronounced for higher values of λ and Ha for the velocity profile. However, for the temperature profile, the effects of these parameters are not prominent. On the other hand, lower values of Pr are more pronounced for the velocity and temperature profiles. In this study, it is also found that the thermal boundary layer thickness reduces when Pr increases for both cases. Dual solutions exist for the opposing flow only for a certain region. There is only a unique solution existed for the assisting flow. It is concluded that the Hartmann number delays the separation of the boundary layer.

References

[1] Ahmad, N., Siddiqui, Z. U., and Mishra, M. K. Boundary layer flow and heat transfer past a stretching plate with variable thermal conductivity. *Int. J. Non-Linear Mech.*, **45**, 306–309 (2010)

[2] Kumari, M. and Nath, G. Unsteady MHD mixed convection flow over an impulsively stretched permeable vertical surface in a quiescent fluid. *Int. J. Non-Linear Mech.*, **45**, 310–319 (2010)

[3] Prasad, K. V., Vajravelu, K., and Datti, P. S. Mixed convection heat transfer over a non-linear stretching surface with variable fluid properties. *Int. J. Non-Linear Mech.*, **45**, 320–330 (2010)

[4] Ali, F. M., Nazar, R., Arifin, N. M., and Pop, I. MHD boundary layer flow and heat transfer over a stretching sheet with induced magnetic field. *Heat and Mass Transfer*, **47**, 155–162 (2011)

[5] Hiemenz, K. Die Grenzschicht an einem in den gleichförmigen Flüssigkeitsstrom eingetauchten geraden Kreiszylinder. *Dingler's Polytech. J.*, **326**, 321–324 (1911)

[6] Eckert, E. R. G. Die Berechnung des Wärmeubergangs in der laminaren Grenzschicht umstromter Körpe. *VDI Forschungsheft*, **416**, 1–23 (1942)

[7] Mahapatra, T. R. and Gupta, A. S. Heat tansfer in stagnation-point flow towards a stretching sheet. *Heat and Mass Transfer*, **38**, 517–521 (2002)

[8] Andersson, H. I. MHD flow of a viscoelastic fluid past a stretching sheet. *Acta Mech.*, **95**, 227–230 (1992)

[9] Ishak, A., Nazar, R., and Pop, I. Magnetohydrodynamic (MHD) flow of a micropolar fluid towards a stagnation point on a vertical surface. *Comp. Math. Appl.*, **56**, 3188–3194 (2008)

[10] Mahapatra, T. R., Nandy, S. K., and Gupta, A. S. Magnetohydrodynamic stagnation-point flow of a power-law fluid towards a stretching surface. *Int. J. Non-Linear Mech.*, **44**, 124–129 (2009)

[11] Gupta, A. S., Pal, A., Pal, B., and Takhar, H. S. Hall effects on MHD flow and heat transfer over a stretching surface. *Int. J. Appl. Mech. Eng.*, **8**, 219–232 (2003)

[12] Ali, F. M., Nazar, R., Arifin, N. M., and Pop, I. Effect of Hall current on MHD mixed convection boundary layer flow over a stretched vertical flat plate. *Meccanica*, **46**, 1103–1112 (2011)

[13] Ishak, A., Nazar, R., and Pop, I. Hydromagnetic flow and heat transfer adjacent to a stretching vertical sheet. *Heat and Mass Transfer*, **44**, 921–927 (2008)

[14] Pop, S. R., Grosan, T., and Pop, I. Radiation effect on the flow near the stagnation point of a stretching sheet. *Technische Mechanik*, **25**, 100–106 (2004)

[15] Pal, D. Heat and mass transfer in stagnation-point flow towards a stretching surface in the presence of buoyancy force and thermal radiation. *Meccanica*, **44**, 145–158 (2009)

[16] Hayat, T., Javed, T., and Abbas, Z. MHD flow of a micropolar fluid near a stagnation-point towards a non-linear stretching surface. *Nonlinear Analysis*: *Real World Applications*, **10**, 1514–1526 (2009)

[17] Shokouhmand, H., Fakoor Pakdaman, M., and Kooshkbaghi, M. A similarity solution in order to solve the governing equations of laminar separated fluids with a flat plate. *Commun. Nonlinear Sci. Numer. Simulat.*, **15**, 3965–3973 (2010)

[18] Vajravelu, K. and Hadijinicolaou, A. Convective heat transfer in an electrically conducting fluid at a stretching surface with uniform free stream. *Int. J. Eng. Sci.*, **35**, 1237–1244 (1997)

[19] Xu, H. An explicit analytic solution for convective heat transfer in an electrically conducting fluid at a stretching surface with uniform free stream. *Int. J. Eng. Sci.*, **43**, 859–874 (2005)

[20] Ishak, A., Jafar, K., Nazar, R., and Pop, I. MHD stagnation point flow towards a stretching sheet. *Physica A*, **388**, 3377–3383 (2009)

[21] Bachok, N., Ishak, A., and Pop, I. Mixed convection boundary layer flow near the stagnation point on a vertical surface embedded in a porous medium with anisotropy effect. *Transport Porous Media*, **82**, 363–373 (2010)

[22] Sutton, G. W. and Sherman, A. *Engineering Magnetohydrodynamics*, McGraw-Hill, New York (1965)

[23] Ramachandran, N., Chen, T. S., and Armaly, B. F. Mixed convection in stagnation flows adjacent to vertical surfaces. *Journal of Heat Transfer*, **110**, 373–377 (1988)

[24] Cebeci, T. and Bradshaw, P. *Physical and Computational Aspects of Convective Heat Transfer*, Springer, New York (1988)

[25] Cebeci, T. and Cousteix, J. *Modeling and Computing of Boundary-Layer Flows*: *Laminar*, *Turbulent and Transitional Boundary Layers in Incompressible and Compressible Flows*, Springer, New York (2005)

[26] Hassanien, I. A. and Gorla, R. S. R. Combined forced and free convection in stagnation flows of micropolar fluids over vertical non-isothermal surfaces. *Int. J. Eng. Sci.*, **28**, 783–792 (1990)

[27] Lok, Y. Y., Amin, N., and Pop, I. Unsteady mixed convection flow of a micropolar fluid near the stagnation point on a vertical surface. *Int. J. Therm. Sci.*, **45**, 1149–1157 (2006)

[28] Ishak, A., Nazar, R., and Pop, I. Dual solutions in mixed convection flow near a stagnation point on a vertical porous plate. *Int. J. Therm. Sci.*, **47**, 417–422 (2008)

[29] Ishak, A., Nazar, R., and Pop, I. Mixed convection boundary layers in the stagnation-point flow towards a stretching vertical sheet. *Meccanica*, **41**, 509–518 (2006)

[30] Rosca, A. V. and Pop, I. Flow and heat transfer over a vertical permeable stretching/shrinking sheet with a second order slip. *Int. J. Heat Mass Transfer*, **60**, 355–364 (2013)

[31] Merkin, J. H. Mixed convection boundary-layer flow on a vertical surface in a saturated porous medium. *J. Eng. Math.*, **14**, 301–313 (1980)

[32] Merkin, J. H. On dual solutions occurring in mixed convection in a porous medium. *J. Eng. Math.*, **20**, 171–179 (1985)

[33] Hoog, F. R., Laminger, B., and Weiss, R. A numerical study of similarity solutions for combined forced and free convection. *Acta Mech.*, **51**, 139–149 (1984)

[34] Afzal, N. and Hussain, T. Mixed convection over a horizontal plate. *Journal of Heat Transfer*, **106**, 240–241 (1984)

[35] Harris, S. D., Ingham, D. B., and Pop, I. Mixed convection boundary-layer flow near the stagnation point on a vertical surface in a porous medium: Brinkman model with slip. *Transport Porous Media*, **77**, 267–285 (2009)